Ceramics-Silikáty 60 (2), 1-11 (2016)
journal webpage: www.ceramics-silikaty.cz doi: 10.13168/cs.2016.0001

LOWERING THE SINTERING TEMPERATURE OF BARIUM STRONTIUM TITANATE BULK CERAMICS BY BARIUM STRONTIUM TITANATE-GEL AND $BaCu(B_2O_5)$

#UWE GLEISSNER*, CHRISTOF MEGNIN*, MANUEL BENKLER*, DANIEL HERTKORN*, HENDRIK C. ELSENHEIMER*, KATRIN SCHUMANN*, FLORIAN PAUL*, THOMAS HANEMANN*, **

*University of Freiburg, IMTEK, Laboratory for Materials Processing, Georges-Köhler-Allee 102, 79110 Freiburg, Germany
**Karlsruhe Institute of Technology (KIT), Institute for Applied Materials - Materials Process Technology, Hermann von Helmholtz Platz 1, 76344 Eggenstein-Leopoldshafen, Germany

#E-mail: uwe.gleissner@imtek.uni-freiburg.de

Submitted November 2, 2015; accepted February 7, 2016

Keywords: Barium strontium titanate (BST), Ferroelectric ceramics, Mixed oxide route, Sol-gel route, Sintering temperature, $BaCu(B_2O_5)$ (BCB), Liquid phase

In this paper the influence of barium strontium titanate (BST) xerogel as a sinter additive and $BaCu(B_2O_5)$ (BCB) as a liquid phase sintering aid on the sintering behavior of BST bulk ceramics is investigated. BST as well as BCB powders were synthesized via a mixed oxide route and BST gel via a sol-gel process. Compared to pure BST bulk ceramics, BST gel reduces the sintering start (onset temperature) by up to 174°C and increases the density for a sintering temperature of 1200°C. By adding BCB to the BST powder the sintering was completed much faster and the onset temperatures were reduced by 281°C and 312°C for 1 mol. % and 2.5 mol. %, respectively. With 2.5 mol. % BCB, the highest density of 96 % (5.41 $g \cdot cm^{-3}$) was achieved at 950°C.

INTRODUCTION

Ferroelectric materials are a sub-group of dielectric materials that show unique physical properties, like piezoelectric or pyroelectric behavior [1]. Furthermore, some of these materials exhibit a change in their relative permittivity (ε_r) with respect to the applied field and are therefore called tunable ferroelectrics. These materials can be used as capacitors in mobile communication systems and wireless techniques such as WiFi, Bluetooth or RFID [2-4]. The operation of many and different wireless communication techniques demands a higher bandwidth or the use of multiband systems [5]. The advantages of tuneable ferroelectrics compared to micro electro mechanical systems (MEMS) are lower power consumption, fast response times, and high Q-values [6-8].

Barium strontium titanate ($Ba_xSr_{1-x}TiO_3$, BST) is such a ferroelectric material and has been the subject of recent research [7, 9, 10, 11]. In this report, the composition $Ba_{0.6}Sr_{0.4}TiO_3$ (BST60) is used, which is known for its high tunability [12]. Dielectric properties of BST can be modified by varying the composition and doping of foreign atoms [13]. There are several production methods for BST like the mixed oxide route (MOX), precipitation, and the sol-gel process [1].

In order to use tuneable ferroelectrics in metal-insulator-metal (MIM)-structures, they have to be contacted by metal electrodes on both sides. The metal electrodes have to be deposited onto the ceramic in the green state and are sintered together with the ceramic material. Typical sintering temperatures for BST are in the range of 1250°C [14] or 1350°C [15], depending on the required density. This leads to a degradation of the metal electrodes and thereby to a decrease of the performance and quality of the corresponding device or application. Therefore, it is necessary to lower the sintering temperature, which then enables the fabrication of MIM structures and the application of LTCC (low-temperature co-fired ceramic) processes.

The sintering temperature of ceramics can be decreased by adding sintering or liquid phase aids. However, despite lowering the sintering temperature, these additives can have a negative impact on ferroelectric properties [16]. In this investigation, BST gel is used as a sintering aid, due to the formation of ceramic particles with a high specific surface area. The high specific area shows an increased sinter activity and, thus, lower sintering temperatures. The organic compounds of BST gel are burned out completely during the sintering process. As a result, no secondary phase is introduced to the BST and no negative influence on the ferroelectric

properties occurs. As a liquid phase aid $BaCu(B_2O_5)$ (BCB) was used, which has low toxicity [17, 18] and is known to lower the sintering temperature of BST down to 950°C [15]. Additionally, a combination of BST gel and BCB was investigated. Table 1 gives an overview of liquid phase sintering additives for BST reported in the literature, the corresponding sintering temperatures and compositions of the BST.

In the next section the experimental part will be described, followed by results and discussion of the experiments and investigated materials and samples. At the end, a short summary, accompanied by the possibility of future applications and prospects, will be presented.

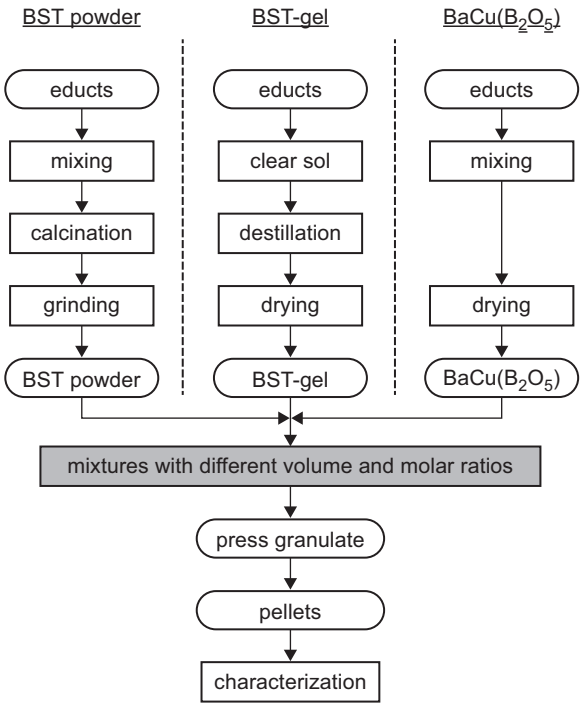

Figure 1. Synthesis routes of BST powder, BST gel and BCB.

EXPERIMENTAL

Figure 1 shows the applied synthesis routes for BST powder, BST gel, and BCB. BST and BCB powder were synthesized via the mixed oxide route [33]. The BST gel was obtained via a sol-gel process [33]. Subsequently the materials were mixed in different volumetric and molar ratios, granulated, and then pressed to pellets.

Synthesis of materials

BST-powder

The BST powder was mixed out of the educts $BaCO_3$ (BDH Prolabo, 99 %), $SrCO_3$ (Alfa Aesar, 99 %), and TiO_2 (Evonik, p25) in the stoichiometric ratio of $Ba_{0.6}Sr_{0.4}TiO_3$. To achieve high homogeneity, the starting materials were mixed using a planetary mill at 200 rpm for 1 h (PM 400/2, Retsch) with 2-Propanol as the dispersing medium and ZrO_2 grinding balls (diameter 1.6 - 1.8 mm). The mixture was then dried in a two-step process using a rotary evaporator (LABOROTA 4003, Heidolph). In the first step 2-Propanol was removed using a water bath at 60°C under 165 mbar pressure to prevent 2-Propanol from boiling. In the second step, the temperature was increased to 75°C and the pressure was lowered to 75 mbar to remove last solvent residues. Afterwards, the grinding balls were removed by sieving. The dried powder was calcined using a ceramic crucible (Al_2O_3) in a chamber furnace (CWF 1300, Carbolite) in ambient air. Doing this, the powder was heated to 1100°C for 2 hours at a rate of 5 $K \cdot min^{-1}$ and subsequently cooled down at the same rate. After calcination, the powder was sieved again, which resulted in ceramic yield of 98 %. To reduce the particle size the powder was ground using a universal roller (UR-1/400-FU-EH, GERMATEC GmbH) for 91 h at 75 rpm. 2-Propanol again was used (volume ratio powder:2-Propanol 1:10)

Table 1. Summary of reported liquid sintering aids, the corresponding sintering temperatures and material compositions of BST.

Additive	Sintering temperature (°C)	Material composition	Reference
Ag	960	BST75	[19]
$BaCuB_2O_5$	950	BST60	[17, 18]
B_2O_3–Li_2CO_3	850	BST60	[20]
B_2O_3	< 1150	BST70	[21]
Bi_2O_3–CuO	975	BST60	[16]
$CuBi_2O_4$	1100	BST60	[22]
CuO	1150	BST50	[23]
Glass frit	900	BST45	[9]
Ba–Sr–Ti–Pb–B–Si–O–Gel-glass	< 1000	BST60	[24]
Bi–Li–glass	920	BST40/50/55/60	[25]
LiO_2	< 900	BST60/55	[26-28]
Li_2CO_3	900	BST50	[29]
Zn–B–Si–O	975	BST70	[30]
ZnBO	1100	BST50	[15, 29, 31, 32]

as a dispersing medium along with ZrO_2 grinding balls (volume ratio powder:balls 1:5) for better grinding. Afterwards the resulting powder was dried as described above and the balls were removed.

BST-gel

The BST gel was synthesized in a temperature controlled glass reactor using the sol-gel route [33]. First, barium acetate (Sigma Aldrich, > 99 %) and strontium acetate (Sigma Aldrich, 97 %) were dissolved in acetic acid at room temperature. After 30 minutes of stirring titanium(IV) isopropoxide, ethylene glycol, and, DI-water were added. The corresponding molar equivalents are given in Table 2.

Table 2. Weighed-in quantities, volumes, and molar equivalents of the educts for the BST-gel.

	Weighed-in quantity (g)	Volume (ml)	Mol equivalent
barium acetate	3.83	1.55	0.6
strontium acetate	2.24	1.07	0.4
titanium alcoholate	7.16	7.375	1.0
acetic acid	39.38	37.50	26.0
ethylene glycol	6.22	5.60	4.0
DI-water	0.45	0.45	1.0

After complete dissolution of all starting materials, the reaction was started by heating up to 150°C at a heating rate of 5 $K \cdot min^{-1}$ and held for 10 h. The solution was then dried at 110°C for 24 h in an oven under an air flow of 5 $l \cdot min^{-1}$.

BCB ($BaCuB_2O_5$)

The liquid phase sintering aid BCB was synthesized by mixing, drying, and calcination of the starting materials barium carbonate, copper oxide, and boric acid, using the process described by Jiang et al. [18]. Mixing was performed according to the BST powder. The precursor was dried using the same rotary evaporator as for BST powder. After drying, the precursor was calcined in a chamber furnace (CWF 1300, Carbolite) inside a crucible (Al_2O_3) at 850°C for 3 h with a heating and cooling rate of 5 $K \cdot min^{-1}$ as well as an air flow of 5 $l \cdot min^{-1}$. Subsequently the powder was ground by hand.

Fabrication of pellets

For dilatometric measurements, pellets with good homogeneity are required. To this end, BST powder, BST gel, and BCB were mixed in a planetary mill with 2-Propanol as a dispersing medium together with ZrO_2 grinding balls. For better handling during the pressing process, 3 vol. % of organic compounds were added consisting of a binder (polyvinylalcohol) and a pressing aid (glycerol). BST gel acts as a pressing aid, so glycerol was only necessary for the formation of pellets without BST gel. To prevent barium ions from dissolving, an aqueous solution of ammonium carbonate was added to all mixtures [34].

To obtain stable pellets with low defect concentrations and high densities, powder mixtures were pre-solidified by uniaxial pressure in a cylinder shaped extrusion die (diameter 20 mm) using a hydraulic press (PW 20 HS, Weber). Here, stearic acid was used as a lubricant. After pre-solidification the powder was pound and finally pressed to pellets by uniaxial pressure in a cylinder shaped extrusion die (diameter 10 mm). The pressing parameters are given in Table 3.

Table 3. Pressing parameters for pre-solidification and the final pellets.

	Pre-solidification	Final pellets
Extrusion die diameter (mm)	20	10
Pressing force (kN)	150	12
Pressure (MPa)	478	153
Pressing time (min)	1	1

BST gel was added to the pellets with different amounts ranging from 0 to 100 vol. %, BCB was added with 1 and 2.5 mol% with respect to the BST content. The compositions of all produced mixtures and pellets are listed in Table 4.

Table 4. Compositions consisting of BST gel, BCB and BCT powder of all investigated mixtures and pellets.

BST gel (vol. %)	BCB (mol. %)	BST powder (vol. %)
0	0	100
0	1	100
0	2.5	100
10	0	90
10	1	90
10	2.5	90
15	0	85
35	0	65
35	1	65
35	2.5	65
50	0	50
73	0	27
84	0	16
100	0	0

Characterization (experimental setup)

The crystalline phase composition of sintered pellets were determined by XRD using a diffractometer (D5000, Siemens) in the Bragg-Brentano geometry.

The exposure wavelength of the monochromatic X-radiation was λ = 1.54 Å (Cu Kα), the anglular range 20 - 60° [35, 36]. The particle size distribution of the BST powder was measured in 2-Propanol using a laser diffraction instrument (LS230, Beckman-Coulter), over a measuring range from 40 nm to 2 mm. Specific surface area was measured using a surface area analyser (Gemini VII 2390, Micromeritics). The density of the produced powders was determined using a helium pycnometer (Pycnomatic ATC, Thermo Scientific). Thermogravimetric and differential thermal analysis (TG-DTA) was performed with 5 K·min^{-1} heating and cooling rates under an ambient air flow of 0.1 l·min^{-1} (STA 409 Jupiter, Netzsch). Dilatometric examination was carried out (Dil 402C, Netzsch) at an air flow of 0.1 l·min^{-1} and heating and cooling rates of 5 K·min^{-1}. Pellet density was analyzed using the Archimedean principle [37, 38]. SEM images were taken (DSM 962, Zeiss) and the quality factor (Q) of the pellets was measured at 1 kHz and room temperature using a precision LCR meter (LCR-800, GW Instek).

RESULTS AND DISCUSSION

Materials

BST powder

The density and specific surface of the BST powder before and after grinding as well as after sintering are shown in Table 5. After grinding, the particle size is smaller and therefore the specific surface area of the powder is increased by a factor of approximately three. Sintering causes density to increase to 5.69 g·cm^{-3}, which is close to the theoretical value of 5.683 g·cm^{-3} found in literature [13]. The D_{50} and D_{90} are given in Table 5 and the particle size distributions of the calcined powders before and after grinding are shown in Figure 2.

BST gel

The sintered density and specific surface of the BST gel were measured after synthesis, pyrolysis, and sintering. The results are listed in Table 6. Compared to the BST powder, the specific surface area of the synthesized BST gel was more than 10 times larger, which results in high activity during sintering. After sintering, the specific surface area was found to be lower compared to BST powder, which confirmed the high sintering activity.

Table 6. Density and specific surface area of BST gel after synthesis, pyrolysis, and sintering.

BST gel	Density (g·cm^{-3})	Specific surface area (m^2·g^{-1})
after synthesis	2.32	196.1
after pyrolysis (450°C, 1 h)	4.20	49.7
after sintering (1200°C, 1 h)	5.61	0.78

Figure 3 shows a TG-DTA measurement of the BST gel. The thermal voltage shows an exothermal peak at a temperature of about 400°C. At this temperature the organic compounds are combusted. Carbonaceous spe-

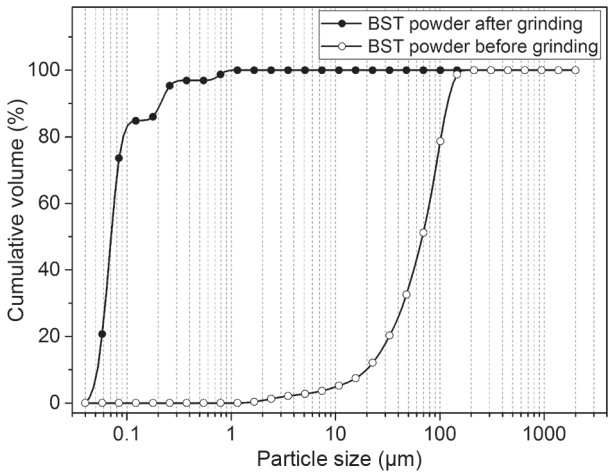

Figure 2. Particle size distribution of calcined BST powder before and after grinding.

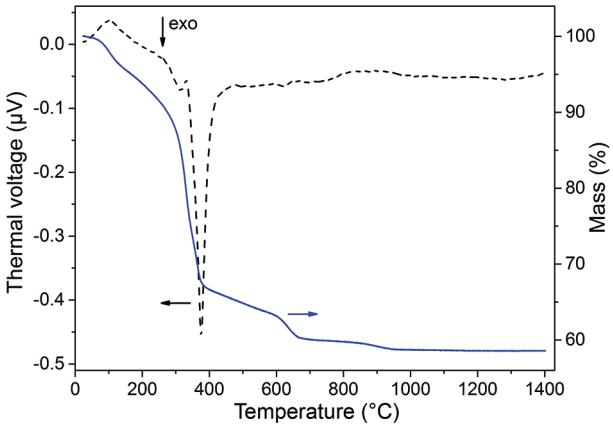

Figure 3. Combined TG-DTA measurement of BST gel under ambient conditions and a temperature up to 1400°C.

Table 5. Density, specific surface, D_{50}, and D_{90} values of synthesized BST powder before and after grinding as well as after sintering.

BST powder	Density (g·cm^{-3})	Specific surface area (m^2·g^{-1})	D_{50} (µm)	D_{90} (µm)
Calcined, before grinding	5.50	5.6	68	118
Calcined, after grinding		17.3	0.07	0.2
After sintering (1200°C, 1h)	5.69	2.8	–	

cies are formed during combustion, which decompose in a two-stage reaction up to 950°C [13]. At this temperature, the mass loss is about 32 % and increases to more than 40 % for 1400°C. The total volume shrinkage of about 80 %, which can be calculated from the mass loss and density, is due to ethylene glycol. After sintering, XRD was carried out (Figure 4), which indicates a slightly higher amount of strontium [25].

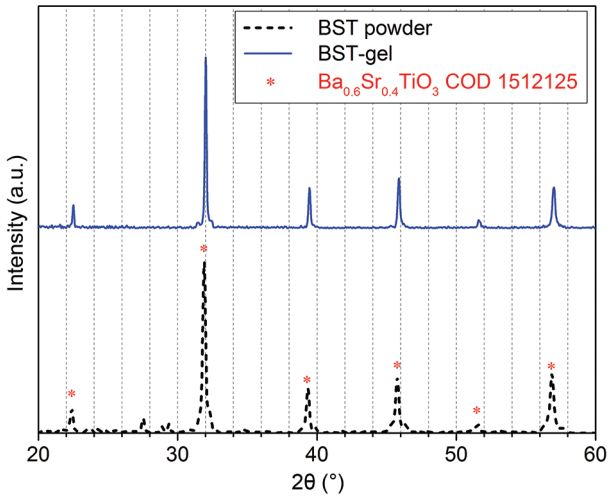

Figure 4. XRD measurement results for BST powder and BST gel and reference out of Crystallography Open Database (COD).

BCB

The synthesized BCB was verified using XRD (Figure 5), and was found to match database values very well. Figure 6 shows TG-DTA measurements of calcined BCB with no mass loss up to 900°C. The melting point is about 890°C, which is lower than the value 930°C reported by Kim et al. [17].

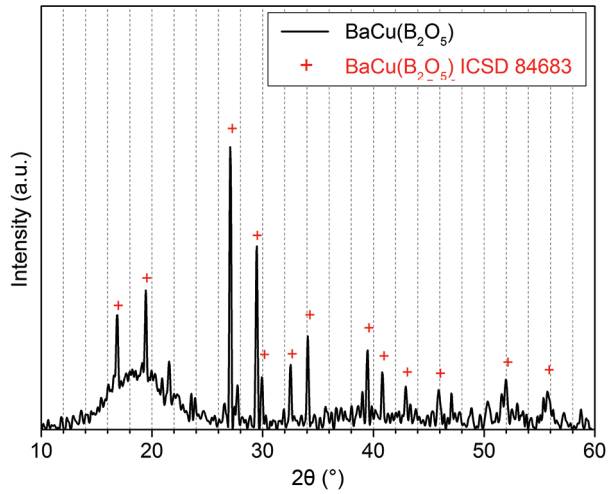

Figure 5. XRD measurement result for $BaCuB_2O_5$ (BCB) powder and reference out of Inorganic Crystal Structure Database (ICSD).

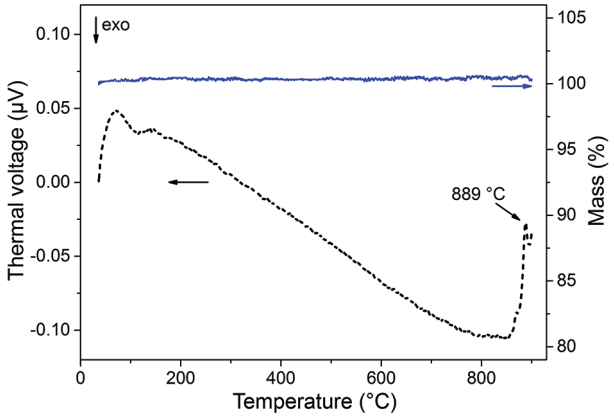

Figure 6. Combined TG-DTA measurement of calcined BCB under ambient conditions for a temperature up to 900°C.

Shrinkage behaviour

BST gel as a sintering aid

Figure 7 compares the temperature dependent shrinkage of different BST powder/BST gel compositions, and shows the suitability of BST gel as a sintering aid. The total shrinkage can be divided into three parts. In part I of Figure 7 ($T < 700$°C), the shrinkage is directly related to the mass loss. In the second part (987°C $< T < 1161$°C) shrinkage is caused by the onset of sintering, mainly as a function of the BST gel content and marked by the grey area. The onset temperatures (Table 7), which indicate the start of sintering, were determined with Proteus Analysis Software (Netzsch) using the tangent method. A higher BST gel concentration results clearly in lower onset temperatures but also in slower shrinkage at higher temperatures. Slower shrinkage is mostly caused by increased porosity and therefore smaller contact surface between the individual ceramic particles. In the third part, sintering slows down for pellets with more than 35 vol. % BST-gel, probably because the high surface area is mainly "consumed" and therefore the driving force of the sintering process is gone.

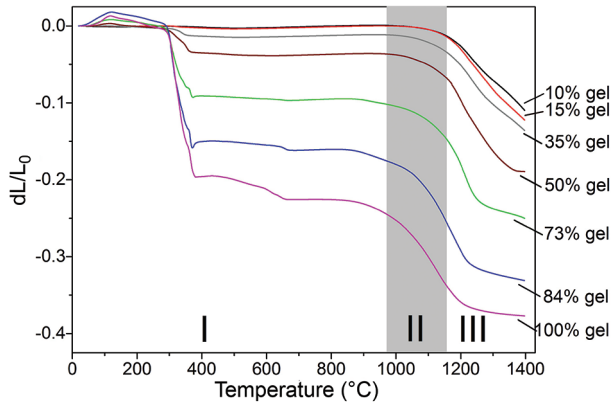

Figure 7. Dilatometric measurements of the linear shrinkage of different BST powder/BST gel mixtures depending on the temperature.

Table 7. Onset temperatures for the different pellets with BST gel, determined with Proteus Analysis Software (Netzsch) using the tangent method.

BST-gel content (vol. %)	Tonset (°C)
0	1161
10	1143
15	1137
35	1130
50	1120
73	1119
84	1043
100	987

BCB as a sintering aid

In Figure 8, the temperature-dependent linear shrinkage for mixtures with 0, 1 and 2.5 mol. % BCB is shown. The sintering behaviour up to 750°C is similar to the mixtures without BCB. The onset temperatures (Table 8) hold an inverse relationship with BCB concentration, decreasing from 880°C for 1 mol.% to 849°C for 2.5 mol.%. Compared to pellets without BCB these onset temperatures are up to 312°C lower. Moreover, shrinkage slope is greater compared to pellets without BCB. Both facts lead to huge advantages realizing maximum densities at low temperatures.

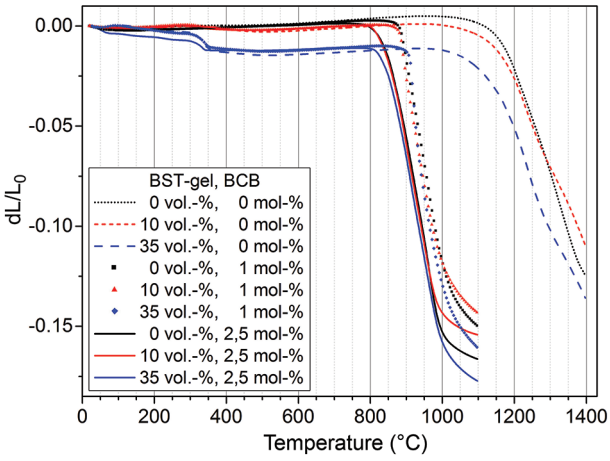

Figure 8. Dilatometric measurements of pellets out of different BST gel and BCB mixtures.

Adding 35 vol. % BST-gel to the mixture with 1 mol. % BCB the onset temperature was increased to 908°C. BST-gel did not influence mixtures with 2.5 mol. % BCB concerning onset temperature. TG-DTA-analysis of the BCB mixtures showed that the shrinkage is only caused by sintering and not due to decomposition of BCB (compare Figure 6).

Table 8. Onset temperatures for the different pellets with BST gel, determined with Proteus Analysis Software (Netzsch) using the tangent method.

BST-gel content (vol. %)	BCB content (mol. %)	T_{onset} (°C)
0	1	880
10	1	879
35	1	908
0	2.5	849
10	2.5	840
35	2.5	845

Density

BST gel as sintering aid

Figure 9 shows relative sinter densities with respect to the theoretical value of BST60 [13], as well as the absolute densities for sintering temperatures up to 1400°C for different contents of BST gel. The sintered density of the pellets depends on the shrinkage during heating and the densification during dwelling time (5 h).

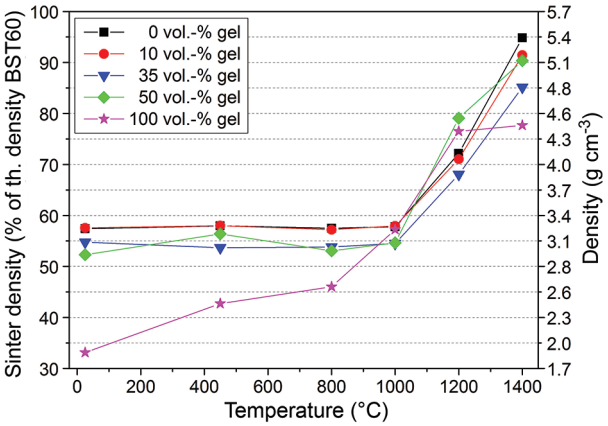

Figure 9. Relative and absolute sinter densities of pellets containing BST-powder and BST-gel, which are sintered at temperatures up to 1400°C for 5 h.

As previously mentioned, BST gel has a very high mass loss below 700°C, resulting in increased porosity. However, simultaneous shrinkage during this phase causes the density to remain constant. Between 1000°C and 1200°C, sinter activity increases greatly (compare onset temperatures – Table 7), resulting in increased density. At 1200°C the high specific surface area of the BST gel is mainly expended and remains constant. Therefore hardly further sintering (compare Figure 7) and accordingly only a slight increase in density is observed. For a sintering temperature of 1400°C the sintered density increases with decreasing BST gel content and shows a maximum for 0 vol. %.

Figure 10 shows the relationship between sintered density and sintering temperature for various amounts of BST gel and two different contents of BCB. The required sintering temperatures are lower due to the use of BCB. At these reduced sintering temperatures, the activation of the high sinter active surface of the BST gel is hampered and therefore no positive effect on the sintering can be seen. For a given temperature, the density increases for a higher content of BCB and lower content of BST gel. For a temperature rise from 875°C to 950°C) the relative density increases from 65 to 82 % for 35 vol. % BST gel and 1 mol. % BCB. By increasing the BCB content to 2.5 mol. % the relative density increases by another 10 %. This behavior is caused by the higher amount of liquid phase (BCB), which leads to faster sintering. Table 9 gives an overview of selected density values of pellets with different BST, BST gel and BCB concentrations sintered at 950°C (1000°C), 1200°C and 1400°C.

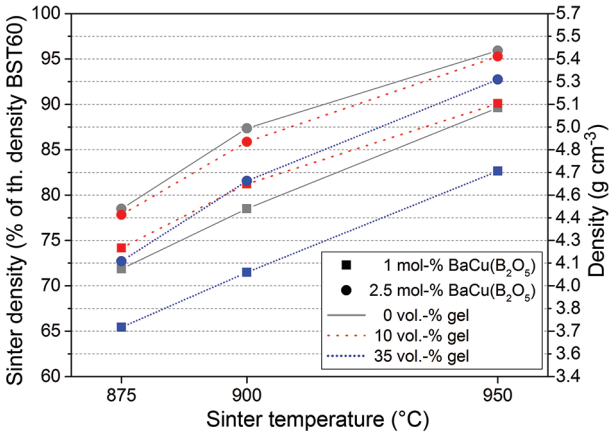

Figure 10. Sinter densities of pellets out of BST powder, BST gel and BCB at different sintering temperatures.

Morphology

SEM pictures were taken to investigate the material structure and grain size of the sintered pellets. In Figure 11 (upper row) pellets with 0 and 35 vol. % BST gel sintered at 1200°C are compared. Both pellets show dense areas, whereas porosity is higher for the pellets containing BST gel. This can also be seen in the density measurements, where the pellet without BST gel shows a higher density at this temperature. In addition, material fragments were pulled out of the bulk due to mechanical erosion during polishing.

SEM pictures of pellets sintered at 1400°C for 5 h illustrate the influence of BST gel on the sintered density. In Figure 11 (lower row) pellets with 0 and 10 vol. % BST gel are shown. 10 vol. % were chosen, because the sample with 35 vol. % BST gel showed no visible grains and also mechanical erosion from polishing. Samples with 0 vol. % BST gel indicate a higher density, even when compared to samples with 10 vol.%, which was also confirmed by measuring the density with the Archimedean principle. They also show closer but bigger grains and less porosity.

SEM pictures of pellets out of pure BST gel sintered at 450, 1200, and 1400°C (top) as well as pellets with BST gel contents of 0, 10, and 35 vol. % with 2.5 mol. % BCB (bottom) are illustrated in Figure 12. Figure 12a shows a pellet sintered at 450°C for 1 h. At this temperature most organic compounds are decomposed. The surface indicates areas of high density but also large breaks and areas of high porosity. Figure 12b and c show samples sintered at 1200°C and 1400°C, respectively. No big difference can be seen as there are dense areas as well as porosity. This result can also be found in Figure 9, where only a small increase in density is shown.

Figure 12 (lower row) shows SEM pictures of pellets with 2.5 mol. % BCB and 0, 10, and 35 vol. % BST gel. The difference between these samples with respect to grain size, density, and porosity is negligible. The reason for this is the low sintering temperature, at which the BST gel is not yet activated. Only the BCB influences the sintering behavior and therefore grain size and density.

Summary of microstructural characteristics

The sintered density of pellets with 50, 73 and 84 vol.% BST gel sintered at 1200°C is higher compared to pellets made from BST powder with a content of BST gel lower than 35 vol. %. At higher temperatures the BST gel showed no advantages with respect to the sintered density. By adding BST gel to the BST powder the onset

Table 9. Overview of selected density values of pellets with different amounts of BST gel and BCB sintered at temperatures in the range of 950 to 1400°C.

BST gel content (vol.%)	BCB content (mol.%)	Density (% of theoretical density)		
		950°C (1000°C)	1200°C	1400°C
0	0	(58)	72	95
50	0	(55)	79	90
100	0	(57)	77	78
0	2.5	96	–	–
10	2.5	95	–	–
35	2.5	93	–	–

temperature decreased with increasing content but the maximum density reached is lower.

Mixtures with BCB as liquid phase sintering aid achieved high densities at low sintering temperatures. Due to the low sintering temperatures which are below the activation temperature of the BST gel, the addition of BST gel to the mixtures with BCB showed no improvements with respect to final density and onset temperatures.

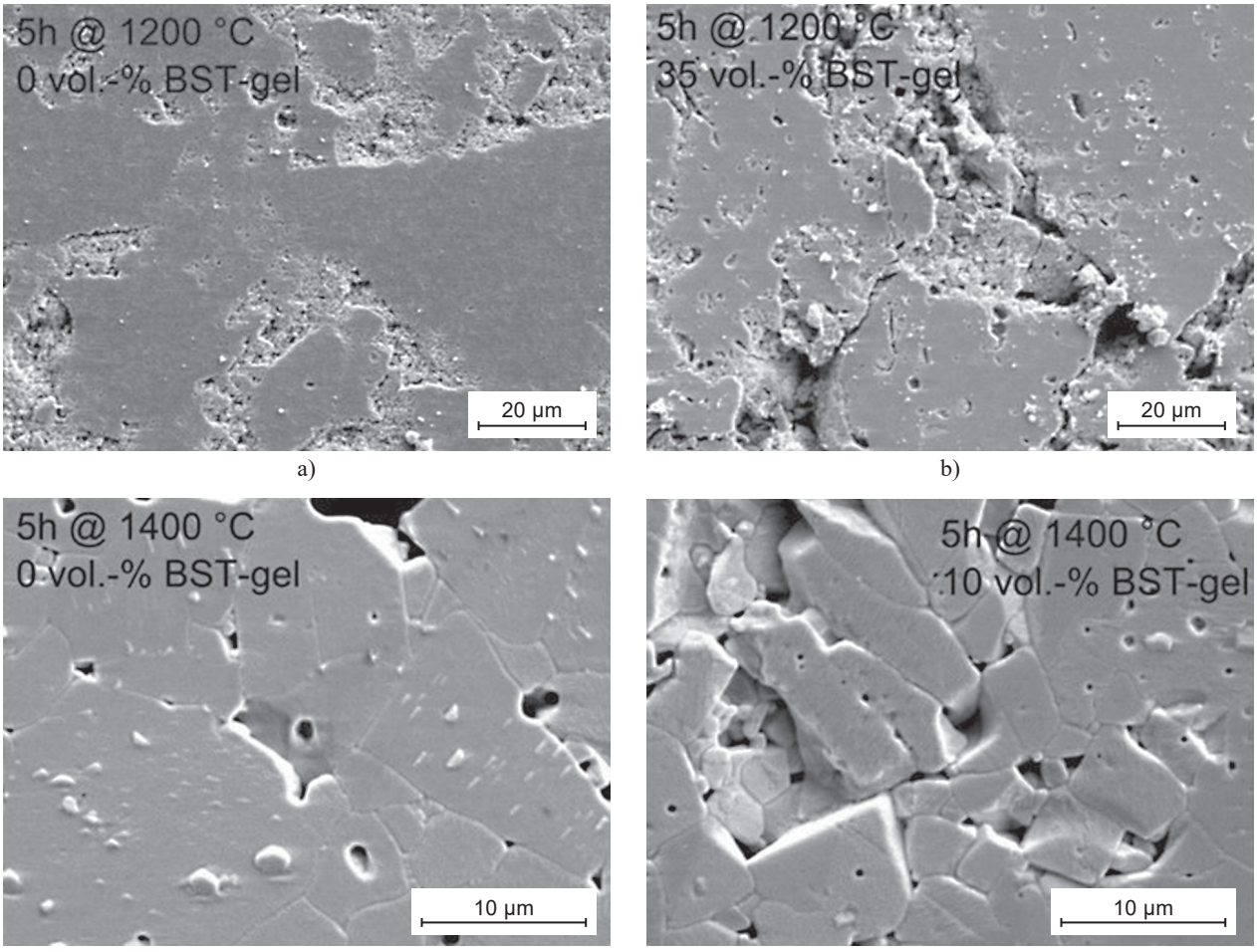

Figure 11. SEM pictures of pellets out of BST powder (a, c) and out of BST powder and 35 vol. % (b) and 10 vol. % BST gel (c) sintered at 1200 (top) and 1400°C (bottom).

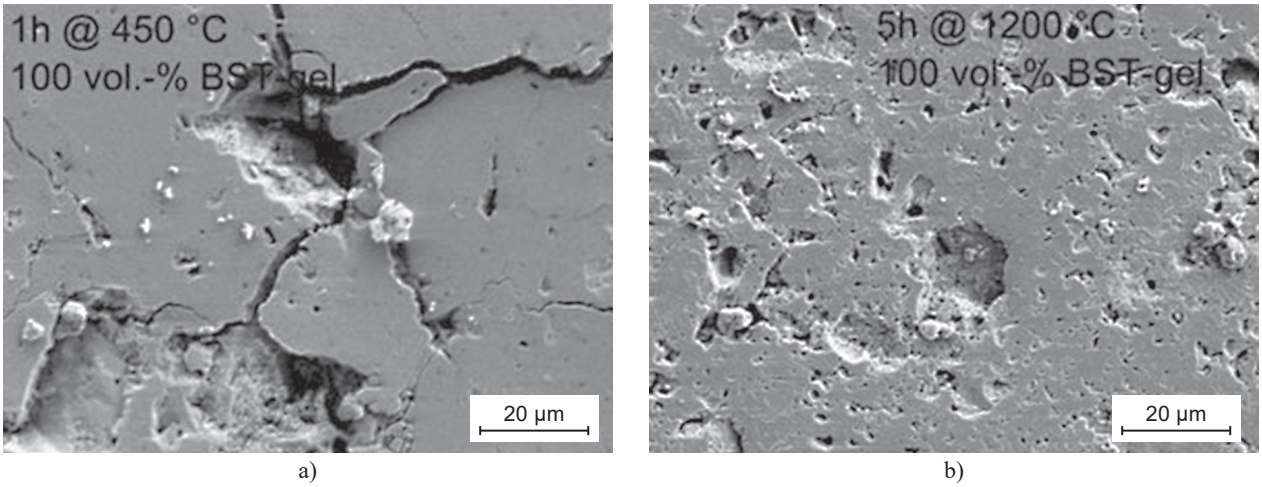

Figure 12. SEM pictures of pellets out of BST gel (top) sintered at 450°C (a), 1200°C (b) and 1400°C (c) and pellets out of BST powder, BCB (bottom) and 0 vol. % (d), 10 vol. % (e) and 35 vol. % (f) BST gel sintered at 950°C and 5 h. *Continue on next page*

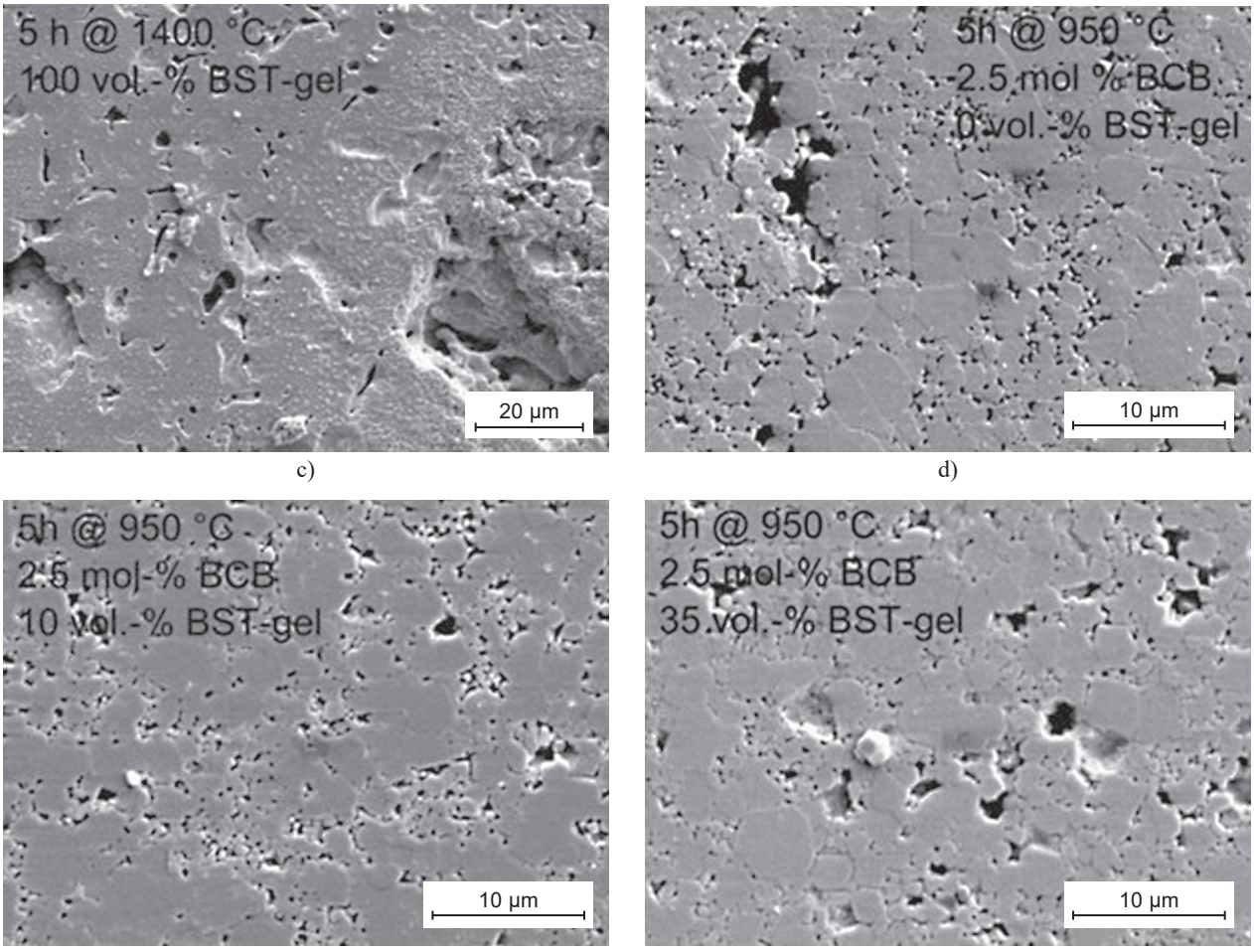

Figure 11. SEM pictures of pellets out of BST powder (a, c) and out of BST powder and 35 vol. % (b) and 10 vol. % BST gel (c) sintered at 1200 (top) and 1400°C (bottom).

Dielectric measurements

Figure 13 shows the influence of different amounts of BST gel and BCB on the quality factor. The quality factor was measured at 1 kHz using a LCR meter. The quality factor increases for lower porosity. This behavior can be seen for samples with increasing content of BST gel with 0 and 1 mol. % BCB. For samples with 2.5 mol. % BCB, the Q-factor shows a minimum for 10 vol. %. These results need further investigation at thick films.

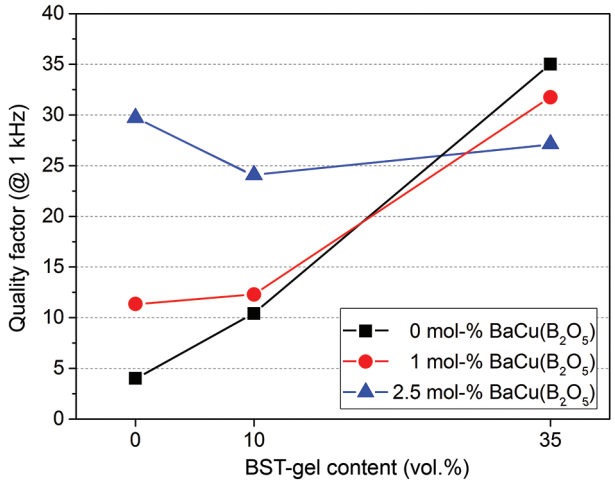

Figure 13. Dielectric measurements of quality factor @ 1 kHz using a LCR meter depending of BCB and BST gel content.

CONCLUSION

In this paper, BST and BCB powders were synthesized using the mixed oxide route, as well as BST gel using a sol-gel process. For the usage of BST gel as a sintering aid, its concentration must be above a threshold of 35 vol. % for it to influence the final density. The onset temperature was seen to decrease by up to 174°C for pure BST gel. For a sintering temperature of around 1200°C and dwelling times of 5 h, the densities of pellets with BST gel are significantly higher compared to the samples without BST gel. At a sintering temperature of 1400°C, these samples could not reach the final density of pure BST powder.

Pellets with BCB reached its maximum density at a sintering temperature of 950°C over a dwelling

time of 5 h. The onset temperature decreased with increasing content of BCB as a liquid phase sintering aid. For 1 mol. % BCB it was possible to reduce the onset temperature by 281°C and with 2.5 mol. % even by 312°C. Overall, sintering occurred much faster when compared to pure BST and therefore much lower temperatures were needed to reach the highest density of 5.41 g·cm^{-3} (96 %). This is very promising compared to other liquid sintering aids like B_2O_3-Li_2CO_3 which only reached 5.22 g·cm^{-3} [20]. Additional BST gel did not reduce the onset temperature or the maximum density any further.

During fabrication of the pellets, the BST gel exhibited a binding effect on the pellets. This could be particularly useful in other fabrication technologies like electrophoretic deposition (EPD), which is used for realization of thick films [39, 40].

Dielectric measurements verified that the quality factor increased with an increasing content of BST gel. Further analysis of the dielectric measurement such as relative dielectric constant and loss tangent vs. temperature at different frequencies is very challenging with bulk ceramics due to the high voltages required. Therefore thick films have to be produced and investigated in the future.

Further progress should also concentrate on a higher ceramic yield of BST gel to prevent high porosity due to organic decomposition. Another possibility could be the pyrolysis of BST gel at 450°C and adding it in different amounts to the mixtures. For this, the described fabrication process of this investigation could be used. The other benefit would be that most of the organic compounds of the BST gel are already decomposed while the specific surface area is still high. This should still lead to a high sinter activity which results then again in high densities.

Acknowledgments

The authors thank Ms. Offermann from Karlsruhe Institute of Technology (KIT, Germany) for measuring powder densities and specific surfaces. The authors also acknowledge financial support by Deutsche Forschungsgesellschaft (DFG).

REFERENCES

1. Haertling G.H. (1999): Ferroelectric ceramics: History and technology. *Journal of the American ceramic society*, *82*(4), 797–818. doi:10.1111/j.1151-2916.1999.tb01840.x.
2. Woong K., Shima H., Yamamoto T., Yasui S., Funakubo H., Yamada T., Nishida K. (2014): Preparation and characterization of ba(zr_xti_{1-x})o_3 thin films for high-frequency applications. *Japanese Journal of Applied Physics*, *53*(9S), doi:09PB04. 10.1143/JJAP.51.09LA01.
3. Tagantsev A.K., Sherman V.O., Astafiev K.F., Venkatesh J., Setter N. (2003): Ferroelectric materials for microwave tunable applications. *Journal of Electroceramics*, *11*(1-2), 5–66. doi:10.1023/B:JECR.0000015661.81386.e6.
4. Kwon S., Hackenberger W., Alberta E., Furman E., Lanagan M. (2011): Nonlinear dielectric ceramics and their applications to capacitors and tunable dielectrics. *Electrical Insulation Magazine, IEEE*, *27*(2), 43–55. doi:10.1109/MEI.2011.5739422.
5. Zhou X. (2012). Prozess- und Dotierungseinflüsse auf $Ba_{0,6}Sr_{0,4}TiO_3$-Dickschichten für steuerbare Mikrowellenkomponenten. Dissertation. Technische Universität Darmstadt, Germany.
6. Babbitt R., Koscica T., Drach W., Didomenico L. (1995): Ferroelectric phase shifters and their performance in microwave phased array antennas. *Integrated Ferroelectrics*, *8*(1-2), 65–76. doi:10.1080/10584589508012301.
7. Zimmermann F., Voigts M., Menesklou W., Ivers-Tiffée E. (2004): $Ba_{0.6}Sr_{0.4}TiO_3$ and $BaZr_{0.3}Ti_{0.7}O_3$ thick films as tunable microwave dielectrics. *Journal of the European Ceramic Society*, *24*, 1729–1733. doi:10.1016/S0955-2219(03)00481-3.
8. Yamada T., Muralt P., Sherman V.O., Sandu C.S., Setter N. (2007) Epitaxial growth of $BaO.3Sr_{0.7}TiO_3$ thin films on Al_2O_3(0001) using ultrathin tin layer as a sacrificial template. *Applied Physics Letters*, *90*(14), 142911. doi:10.1063/1.2719673.
9. Zhang D., Hu W., Meggs C., Su B., Price T., Iddles D., Lancaster M.J., Button T.W. (2007): Fabrication and characterization of barium strontium titanate thick film device structures for microwave applications. *Journal of the European Ceramic Society*, *27*(27), 1047–1051. doi:10.1016/j.jeurceramsoc.2006.05.051.
10. Oh S.-W., Park J.-H., Akedo J. (2007). Dielectric characterization of barium strontium titanate (bst) films prepared on cu substrate by aerosol deposited method, in *Sixteenth IEEE International Symposium on Applications of Ferroelectrics*. ISAF. pp. 207–208.
11. Jeon J.-H. (2004): Effect of $SrTiO_3$ concentration and sintering temperature on microstructure and dielectric constant of $Ba_{1-x}Sr_xTiO_3$. *Journal of the European Ceramic Society*, *24*(6), 1045–1048. doi:10.1016/S0955-2219(03)00385-6.
12. Zimmermann F., Voigts M., Weil C., Jakoby R., Wang P., Menesklou W., Ivers-Tiffee E. (2001): Investigation of barium strontium titanate thick films for tunable phase shifters. *Journal of the European Ceramic Society*, *21* (10-11), 2019–2023. doi:10.1016/S0955-2219(01)00164-9.
13. Paul F. (2006). Dotierte $Ba_{0,6}Sr_{0,4}TiO_3$-Dickschichten als steuerbare Dielektrika. PhD thesis. University of Freiburg, Germany.
14. Su B., Button T. (2001): The processing and properties of barium strontium titanate thick films for use in frequency agile microwave circuit applications. *Journal of the European Ceramic Society*, *21*(15), 2641–2645. doi:10.1016/S0955-2219(01)00330-2.
15. Kim S., Koh J.-H. (2009) Dielectric Properties of ZnBO doped (Ba,Sr)TiO_3 Ceramics for the low temperature sintering process. *Integrated Ferroelectrics*, *110*(1), 17–24. doi:10.1080/10584580903435273.
16. Jiang H., Zhai J., Zhang J., Yao X. (2009): Dielectric Properties of Low-Temperature Sintered $BaO_{.6}Sr_{O.4}TiO_3$ Ceramics by Addition of Bi_2O_3-CuO Mixed Oxides. *Key Engineering Materials*, *421-422*, 61–64. doi:10.4028/www.scientific.net/KEM.421-422.61.

17. Kim M., Lim J., Kim J.-C., Nahm S., Paik J.-H., Kim J.-H., Park K.-S. (2006): Synthesis of $BaCu(B_2O_5)$ Ceramics and their Effect on the Sintering Temperature and Microwave Dielectric Properties of $Ba(Zn_{1/3}Nb_{2/3})O_3$ Ceramics. *Journal of the American Ceramic Society*, *89*(10), 3124–3128. doi:10.1111/j.1551-2916.2006.01157.x.
18. Jiang H., Zhai J., Zhang J., Yao X. (2009): Microwave Dielectric Properties and Low-Temperature Sintering of $Ba_{0.6}Sr_{0.4}TiO_3$ Ceramics. *Journal of the American Ceramic Society*, *92*(10), 2319–2322. doi:10.1111/j.1551-2916.2009.03226.x.
19. Huang J., Cao Y., Hong M., Du P. (2008): Ag–$Ba_{0.6}Sr_{0.4}TiO_3$ composites with excellent dielectric properties. *Applied Physics Letters*, *92*(2), 022911. doi:10.1063/1.2836764.
20. Li, M. Yu Q., Qian K., Ji S., Du P. (2011): The Effect of B_2O_3-Li_2CO_3 Addition on Sintering Behavior and Dielectric Properties of $Ba_{0.6}Sr_{0.4}TiO_3$ Ceramics. *Advanced Materials Research*, *197-198*, 333–338. doi:10.4028/www.scientific.net/AMR.197-198.333.
21. Rhim S., Hong S., Bak H., Kim O. (2000): Effects of B_2O_3 Addition on the Dielectric and Ferroelectric Properties of $Ba_{0.7}Sr_{0.3}TiO_3$ Ceramics. *Journal of the American Ceramic Society*, *83*(5), 1145–1148. doi:10.1111/j.1151-2916.2000.tb01345.x.
22. Jiang H., Zhai J., Chou X., Yao X. (2009): Influence of Bi_2O_3 and CuO addition on low-temperature sintering and dielectric properties of $Ba_{0.6}Sr_{0.4}TiO_3$ ceramics. *Materials Research Bulletin*, *44*(3), 566–570. doi:10.1016/j.materresbull.2008.07.016.
23. Yun S.-W., Koo S.-M., Ha J.-G Koh J.-H. (2010): Influence of CuO Addition to $(Ba_{0.5}Sr_{0.5})TiO_3$ Ceramics on Sintering Behavior and Dielectric Properties. *Ferroelectrics*, *403*(1), 19–25. doi:10.1080/00150191003744583.
24. Wu B., Zhang L., Yao X. (2004): Low temperature sintering of $Ba_{0.6}Sr_{0.4}TiO_3$ glass-ceramic. *Ceramics International*, *30*(7), 1757 – 1761. doi:10.1016/j.ceramint.2003.12.130.
25. Jiang H., Zhai J., Chou X., Yao X. (2010) ?. Microwave Property of Low-Temperature-Sintered $Ba_{1-x}Sr_xTiO_3$ Ceramics with B-Li Glass Sintering Aid. *Ferroelectrics*, *403*(1), 11–18. doi:10.1080/00150191003744492.
26. Zhang M., Wang H., Yang H., Liu W., Zhou H., Yao X. (2011): Enhanced dielectric properties of low-temperature-sintered $Ba_{0.6}Sr_{0.4}TiO_3$ thick films. *Journal of Electroceramics*, *26*, 99–104. doi:10.1007/s10832-011-9634-y.
27. Valant M., Suvorov D. (2004): Low-Temperature Sintering of (Ba0,6Sr0,4)TiO3. *Journal of the American Ceramic Society*, *87*(7), 1222–1226. doi:10.1111/j.1151-2916.2004.tb07716.x.
28. Tick T., Peräntie J., Jantunen H., Uusimäki A. (2008): Screen printed low-sintering-temperature barium strontium titanate (BST) thick films. *Journal of the European Ceramic Society*, *28*(4), 837–842. doi:10.1016/j.jeurceramsoc.2007.08.008.
29. Kim S.-H., You H.-W., Koo S.-M., Ha J.-G., Nam S.-M., Koh J.-H., Jeong S. J. (2009): Comparative Analysis of Li_2CO_3 Doped (Ba,Sr)TiO_3 and ZnBO Doped (Ba,Sr)TiO_3 Ceramics for the Low Temperature Sintering Applications. *Ferroelectrics*, *382*(1), 76–84. doi:10.1080/00150190902869863.
30. Wu B., Zhang L., Yao X. (2004): The effect of Zn-B-Si-O addition on $Ba_{0.7}Sr_{0.3}TiO_3$ by sol-gel process. *Ceramics International*, *30*(7), 1753 – 1756. doi:10.1016/j.ceramint.2003.12.132.
31. Kim S.-H., Koh J.-H. (2008): ZnBO-doped (Ba, Sr) TiO_3 ceramics for the low-temperature sintering process. *Journal of the European Ceramic Society*, *28*, 2969–2973. doi:10.1016/j.jeurceramsoc.2008.04.034.
32. Kim S.-H., Koh J.-H. (2009): Dielectric Properties and AC Conduction of 5 wt. % ZnBO Doped (Ba,Sr)TiO_3 Ceramics for Low Temperature Co-fired Ceramics Applications. *Japanese Journal of Applied Physics*, *48*(4), 041407. doi:10.1143/JJAP.48.041407.
33. Hilton A.D., Frost R. (1992): Recent developments in the manufacture of barium titanate powders. *Key Engineering Materials*, *66-67*, 145–184. doi:10.4028/www.scientific.net/KEM.66-67.145.
34. Neubrand A., Lindner R., Hoffmann P. (2000): Room-temperature solubility behavior of barium titanate in aqueous media. *Journal of the American Ceramic Society*, *83*(4), 860–864. doi:10.1111/j.1151-2916.2000.tb01286.x.
35. Deutsches Zentrum für Luft- und Raumfahrt – Institut für Werkstoff-Forschung. Institutsbroschüre: Mikroanalytik, Metallographie und werkstoffmechanische Prüfung, http://www.dlr.de/wf/portaldata/23/resources/dokumente/flyers/mum/mikroanalytik-metallographie-werkstoff-mechanische_pruefung.pdf. Version of 12/08/07.
36. MRL Frederick Seitz Materials Research Laboratory. http://mrl.illinois.edu/facilities/center-microanalysis-materials/cmm-instruments/x-ray-diffraction-xrd-and-reflectivity-xrr. Version of 12/08/07.
37. DIN EN 993-1. Prüfverfahren für dichte geformte feuerfeste Erzeugnisse. Teil1: Bestimmung der Rohdichte, offenen Porosität und Gesamtporosität, 1995.
38. DIN EN 623-2. Monolithische Keramik – Allgemeine und strukturelle Eigenschaften. Teil 2: Bestimmung von Dichte und Porosität, 1993.
39. Ngo E., Joshi P. C., Cole M. W., Hubbard C. W. (2001): Electrophoretic deposition of pure and MgO-modified $Ba_{0.6}Sr_{0.4}TiO_3$ thick films for tunable microwave devices. *Applied Physics Letters*, *79*(2), 248-250. doi:10.1063/1.1384899.
40. Guo H., Gao W., Yoo J. (2004): Barium strontium titanate ($Ba_{0.7}Sr_{0.3}TiO_3$) ferroelectric films produced by electrophoretic deposition. *Current Applied Physics*, *4*(2), 385-388. doi:10.1016/j.cap.2003.11.055.